

# Clearance of senescent cells with ABT-263 improves biological functions of synovial mesenchymal stem cells from osteoarthritis patients

Kentaro Endo (✉ [endo.arm@md.tmd.ac.jp](mailto:endo.arm@md.tmd.ac.jp))

Tokyo Medical and Dental University: Tokyo Ika Shika Daigaku <https://orcid.org/0000-0003-4790-4632>

Yugo Miura

Tokyo Medical and Dental University: Tokyo Ika Shika Daigaku

Keiichiro Komori

Tokyo Medical and Dental University: Tokyo Ika Shika Daigaku

Ichiro Sekiya

Tokyo Medical and Dental University: Tokyo Ika Shika Daigaku

---

## Research Article

**Keywords:** Mesenchymal stem cells, senescence, senolytic drug, osteoarthritis, ABT-263, synovium

**Posted Date:** March 3rd, 2022

**DOI:** <https://doi.org/10.21203/rs.3.rs-1402507/v1>

**License:**  This work is licensed under a Creative Commons Attribution 4.0 International License.

[Read Full License](#)

---

1   **Clearance of senescent cells with ABT-263 improves biological functions of**  
2   **synovial mesenchymal stem cells from osteoarthritis patients**

3

4   Yugo Miura, Kentaro Endo\*, Keiichiro Komori, Ichiro Sekiya

5

6   Center for Stem Cell and Regenerative Medicine, Tokyo Medical and Dental

7   University, Tokyo, Japan

8

9   Corresponding author: Kentaro Endo

10   Project Assistant Professor, Center for Stem Cell and Regenerative Medicine,

11   Tokyo Medical and Dental University (TMDU)

12   1-5-45 Yushima, Bunkyo-ku, Tokyo, 113-8510, Japan

13   Tel: +81-3-5803-4017

14   Email: [endo.arm@tmd.ac.jp](mailto:endo.arm@tmd.ac.jp)

15     **Abstract**

16     **Background:** Osteoarthritis (OA) is an age-related joint disease characterized  
17     by progressive cartilage loss. Synovial mesenchymal stem cells (MSCs) are  
18     anticipated as a cell source for OA treatment; however, synovial MSC  
19     preparations isolated from OA patients contain many senescent cells that inhibit  
20     cartilage regeneration through their senescence-associated secretory phenotype  
21     (SASP) and poor chondrogenic capacity. The aim of this study was to improve  
22     the biological function of OA synovial MSCs by removing senescent cells using  
23     the senolytic drug ABT-263.

24     **Methods:** We pretreated synovial MSCs derived from 5 OA patients with ABT-  
25     263 for 24 h and then evaluated senescence-associated beta galactosidase (SA-  
26      $\beta$  gal) activity, apoptosis, surface antigen expression, colony formation ability, and  
27     multipotency.

28     **Results:** The ABT-263 pretreatment significantly decreased the percentage of  
29     SA- $\beta$  gal-positive cells and induced early- and late-stage apoptosis. Cleaved  
30     caspase-3 was expressed in SA- $\beta$  gal-positive cells. The pretreated MSCs  
31     formed greater numbers of colonies with larger diameters. The expression rate  
32     of CD34 was decreased in the pretreated cells. Differentiation assays revealed

33 that ABT-263 pretreatment enhanced the adipogenic and chondrogenic  
34 capabilities of OA synovial MSCs. In chondrogenesis, the pretreated cells  
35 produced greater amounts of glycosaminoglycan and showed lower expression  
36 of senescence markers (p16 and p21) and SASP factors (MMP-13 and IL-6).

37 **Conclusion:** Pretreatment of synovial MSCs from OA patients with ABT-263 can  
38 improve the function of the cells by selectively eliminating senescent cells. These  
39 findings indicate that ABT-263 could hold promise for the development of effective  
40 cell-based OA therapy.

41

42 **Keywords**

43 Mesenchymal stem cells, senescence, senolytic drug, osteoarthritis, ABT-263,  
44 synovium.

45

46 **Background**

47 Knee osteoarthritis (OA) is the most common joint disease worldwide. It  
48 is characterized by a progressive loss of articular cartilage and meniscus  
49 degeneration associated with aging and synovitis [1] and has recently been  
50 designated an age-related inflammatory disease [2]. OA patients suffer from a

51 variety of symptoms (e.g., pain, stiffness, swelling, and loss of mobility), so the  
52 recommended therapies can range from pain control to surgery [3]. However,  
53 none of the available treatments can improve cartilage loss sufficiently to affect  
54 patients fundamentally. New treatments are therefore needed to overcome this  
55 limited effectiveness, because the number of OA patients is anticipated to  
56 increase in today's aging society.

57 One promising OA treatment that has emerged in the last two decades is  
58 the use of mesenchymal stem cells (MSCs). These cells are considered a viable  
59 therapeutic alternative for OA due to their pleiotropic abilities, such as self-  
60 renewal, multipotency, and secretion of cytokines and growth factors [4, 5]. MSCs  
61 can be obtained from various tissues, but synovial MSCs have a higher colony  
62 formation ability and chondrogenic potential than MSCs from other tissues, and  
63 are therefore promising for treating damaged cartilage [6-9]. We previously  
64 demonstrated that synovial MSCs transplanted into rabbit cartilage or meniscus  
65 defects could promote regeneration by producing abundant cartilage matrices [10,  
66 11]. Similarly, intra-articular injection of synovial MSCs suppressed the  
67 progression of OA in rats [12]. Our recent clinical study in human OA patients  
68 showed that transplantation of autologous synovial MSCs improved the clinical

69 outcomes and the amounts of cartilage that could be assessed by automatic  
70 magnetic resonance imaging (MRI) [13].

71 One issue with the use of MSCs as an OA treatment is that the MSC  
72 preparations typically contain senescent cells. Senescence in cells, including  
73 MSCs, is triggered by some type of stress that causes the activation of the p16  
74 or p21 pathways. This puts the cells into permanent cell-cycle arrest, resulting in  
75 resistance to apoptosis [14]. The senescent cells remain metabolically active and  
76 release factors referred to as senescence-associated secretory phenotype  
77 (SASP) factors, which include proinflammatory cytokines (e.g., interleukin-6; IL-  
78 6) and proteinases (e.g., matrix metalloprotease-13; MMP-13) [14]. SASP plays  
79 a crucial role in accelerating the senescence of other neighboring cells and  
80 deteriorating their function[14].

81 In OA knees, chondrocyte senescence can be induced by a number of  
82 different stresses [1], and recent reports indicate that senescent cells also  
83 accumulate in the OA synovium and in the MSCs isolated from it [15, 16]. This  
84 means that senescent cells are also present in cultures of synovial MSCs that are  
85 used as OA therapeutics. The cultures containing senescent MSCs lack full OA  
86 therapeutic efficacy due to their release of SASP factors and their poor

87 chondrogenic capacity [16]. Therefore, clearance of senescent cells from MSC  
88 cultures intended for therapeutic use is necessary to maximize the efficacy of OA  
89 synovial MSCs.

90 Senescent cells can be selectively removed from cultures by drugs  
91 known as senolytics. Several senolytics have been introduced in several previous  
92 reports; however, ABT-263 (Navitoclax) is one of the best studied of these  
93 senolytic drugs. ABT-263 is an inhibitor of the anti-apoptotic proteins of the BCL-  
94 2 protein family, and its suppression of BCL-2 activity can induce senescent cells  
95 in various tissues to undergo apoptosis [17]. Grezella et al. demonstrated that  
96 ABT-263 exerted a senolytic effect in replicative senescent human bone marrow  
97 derived MSCs [18]. However, no studies have yet focused on the use of ABT-263  
98 for the qualitative alteration of MSCs, and little is known about the effects of this  
99 drug on senescent OA synovial MSCs.

100 Our aim in the present study was to use ABT-263 to selectively eliminate  
101 senescent cells from synovial MSC samples derived from patients with OA as a  
102 way to improve the quality of MSCs used for OA therapy. We pretreated OA  
103 synovial MSCs with ABT-263 for a short period and then evaluated the extent of  
104 senescent cell clearance and the in vitro biological potencies of the treated MSC

105 samples.

106

107 **Methods**

108 **Isolation of human synovial MSCs**

109 Human synovial samples were acquired from 5 OA donors (age range  
110 71–80 years; one male and four females) who underwent total knee arthroplasty.  
111 The synovium was digested with 3 mg/mL collagenase (Sigma-Aldrich, Saint  
112 Louis, MO, USA) at 37 °C for 3 h. Debris was then removed by passing the digest  
113 through a 70 µm cell strainer (Greiner Bio-One, Kremsmünster, Austria) and the  
114 filtrate was collected. The cells were washed with phosphate buffered saline  
115 (PBS), and the nucleated cells were counted and plated in 145 cm<sup>2</sup> dishes at a  
116 density of 2,000 cells/cm<sup>2</sup> in a growth medium consisting of α-modified essential  
117 medium (α-MEM; Thermo Fisher Scientific, Waltham, MA, USA) and 10% fetal  
118 bovine serum (Thermo Fisher Scientific), and 1% antibiotic-antimycotic (Thermo  
119 Fisher Scientific). After 2 weeks of culture, the cells were detached with 0.25%  
120 trypsin and 1 mM EDTA (Thermo Fisher Scientific) and then cryopreserved in  
121 growth medium supplemented with 5% dimethyl sulfoxide (DMSO; Wako, Tokyo,  
122 Japan).

123

124 **Pretreatment with ABT-263**

125 ABT-263 was obtained from MedChemExpress (Monmouth Junction, NJ,

126 USA). Human synovial MSCs at passage 1 were used for all experiments. The

127 cells were treated for 24 h with 0.1% DMSO (control group) or with 20 µM ABT-

128 263 in DMSO (ABT-263 group). After the treatment, the culture medium was

129 changed to the growth medium, and the cells were further expanded for 6 days.

130 Apoptosis assays were performed immediately after the treatment. An

131 experimental scheme is shown in Fig. 1.

132

133 **Senescence associated-β galactosidase (SA-β-gal) staining**

134 SA-β-gal staining was performed using a Senescence β-Galactosidase

135 Staining Kit (Cell Signaling Technology, Danvers, MA, USA), according to the

136 manufacturer's instructions. Briefly, the cells were fixed with fixative solution and

137 then incubated at 37 °C in staining solution at pH 6.0 for 16 h. Senescent cells

138 were identified as blue-stained cells under brightfield microscopy. Cells positive

139 for SA-β-gal staining were counted manually in four fields at ×10 magnification.

140

141     **Apoptosis assay**

142                 Human synovial MSCs were treated with 0.1% DMSO or 20 µM ABT-263  
143                 for a day. After the treatment, the cells were detached with trypsin, suspended in  
144                 PBS, and the cell suspension was incubated with FITC-annexin V and propidium  
145                 iodide (PI) using an FITC-Annexin V Apoptosis Detection Kit (BD Biosciences,  
146                 NJ, USA). The fluorescence intensity was evaluated using a FACSVerse II  
147                 system (BD Biosciences). The obtained data were analyzed using FlowJo version  
148                 8.7.1 (Ashland, OR, USA).

149

150     **Co-staining of SA-β gal and cleaved caspase-3**

151                 Human synovial MSCs were cultured in 8-well chamber slides (Thermo  
152                 Fisher Scientific). The cells were treated for 6 h with ABT-263 and then stained  
153                 for SA-β gal. The cells were fixed with 4% paraformaldehyde (Sigma-Aldrich),  
154                 permeabilized, and blocked with 0.3% Triton and 5% normal goat serum. The  
155                 cells were then incubated overnight at 4 °C with antibody against cleaved  
156                 caspase-3 (1:400; Cell Signaling Technology). After three washes with PBS, the  
157                 cells were incubated with anti-rabbit secondary antibodies with horseradish  
158                 peroxidase (Abcam, Cambridge, UK) for 1 h at room temperature.

159 Diaminobenzidine (DAB) solution (Dako North America, Carpinteria, CA, USA)

160 was applied for 10 min.

161

162 **Colony-forming assays**

163 Cells pretreated with ABT-263 were seeded at 100 cells/dish in 145 cm<sup>2</sup>

164 dishes (Thermo Fisher Scientific) and cultured for 2 weeks. The cells were then

165 fixed with 10% neutral buffered formalin (Muto Pure Chemicals, Tokyo, Japan),

166 followed by staining with 0.5% crystal violet (Wako). Colonies were counted

167 manually, and the diameter was assessed by Image J (National Institute of Health,

168 Bethesda, MD, USA). Colonies less than 2 mm in diameter and faintly stained

169 colonies were ignored.

170

171 **Surface antigens**

172 Human synovial MSCs were detached with trypsin and suspended in

173 PBS containing 2% FBS and 5 mM EDTA. The MSCs were then stained for 30

174 min at 4 °C with CD44-APCH7, CD73-V450, CD90-PE-Cy7, CD105-APC, CD34-

175 PE, and CD45-PerCP-Cy5.5 antibodies (BD Biosciences), using Ghost Dye

176 Violet (Tonbo Biosciences, San Diego, CA, USA) to remove dead cells. Isotype

177 controls were prepared as negative controls. The percentage of antigen-positive  
178 cells was evaluated using a FACSVerse II system (BD Biosciences).

179

180 **Differentiation assays**

181 For adipogenesis, 100 pretreated human synovial MSCs were plated in  
182 10 cm dishes (Thermo Fisher Scientific) and cultured for 14 days to form colonies.  
183 The adherent cells were then cultured for an additional 21 days in an adipogenic  
184 induction medium consisting of growth medium supplemented with 100 nM  
185 dexamethasone (Wako), 0.5 mM isobutylmethylxanthine (Sigma-Aldrich), 50 mM  
186 indomethacin (Sigma-Aldrich), 4.5 mg/mL D-(+)-glucose (Wako), and 10 µg/mL  
187 recombinant human insulin (Wako). The cells were then fixed with 10% neutral  
188 buffered formalin and stained with oil red O (Sigma-Aldrich), and the oil red O-  
189 positive colonies were counted manually. Each dish was then stained with 0.5%  
190 crystal violet to determine the percentage of oil red O-positive colonies.

191 Osteogenesis assays were performed by plating 100 pretreated MSCs in  
192 10 cm dishes and culturing for 14 days to form colonies. Adherent cells were then  
193 cultured in an osteogenic induction medium consisting of growth medium  
194 supplemented with 50 µg/mL ascorbic acid 2-phosphate (Wako), 1 nM

195 dexamethasone, and 10 mM  $\beta$ -glycerophosphate (Sigma-Aldrich). After 21 days,  
196 the cells were fixed with 10% neutral buffered formalin and stained with alizarin  
197 red (Sigma-Aldrich). The alizarin red-positive colonies were counted manually.  
198 Each dish was then stained with 0.5% crystal violet to determine the percentage  
199 of alizarin red-positive colonies.

200 For chondrogenesis,  $2.5 \times 10^5$  pretreated MSCs were transferred to a 15  
201 mL polypropylene tube (Thermo Fisher Scientific) and centrifuged at  $580 \times g$  for  
202 10 min. The pelleted cells were then cultured in chondrogenic induction medium  
203 consisting of high glucose Dulbecco's Modified Eagle Medium (Thermo Fisher  
204 Scientific), 1 % insulin-transferrin-selenium (ITS; BD Biosciences), 50  $\mu\text{g/mL}$   
205 ascorbate-2-phosphate, 40  $\mu\text{g/mL}$  L-proline (Sigma Aldrich), 100 nM  
206 dexamethasone, 100  $\mu\text{g/mL}$  pyruvate (Sigma Aldrich), 1 % antibiotic-antimycotic,  
207 10 ng/mL transforming growth factor- $\beta$ 3 (Miltenyi Biotec, Bergisch Gladbach,  
208 Germany), and 500 ng/mL bone morphogenetic protein-2 (Medtronic,  
209 Minneapolis, MN, USA). After 3 weeks of cultivation in a chondrogenic induction  
210 medium, 5-6 pellets in each group were weighed. Two pellets each were fixed in  
211 10% neutral buffered formalin, embedded in paraffin, and cut into 5  $\mu\text{m}$  thick  
212 sections. The sections were stained with safranin O (Chroma Gesellschaft

213 Schmid & Co., Munster, Germany) and fast green (Wako) to evaluate the  
214 production of Glycosaminoglycan (GAG). Three or four pellets each were used  
215 for biochemical analysis.

216

217 **Biochemical analysis**

218 GAG and deoxyribonucleic acid (DNA) were quantified by digesting the  
219 pellets with 100 µg/mL papain (Sigma-Aldrich) at 65°C for 16 h. DNA content was  
220 measured using Hoechst 33258 dye (Dojindo, Tokyo, Japan). Fluorescence  
221 intensity was measured with a microplate reader (Tecan, Männedorf,  
222 Switzerland) at an excitation wavelength of 360 nm and an emission wavelength  
223 of 465 nm. Calf thymus DNA (Sigma-Aldrich) was used to generate a standard  
224 curve. The GAG content was then quantified with a Blyscan Kit (Biocolor,  
225 Westbury, NY, USA) according to the manufacturer's instructions. The optical  
226 density was measured at 656 nm with a microplate reader, and the total GAG  
227 content was calculated. For comparison of the GAG-producing ability, the GAG  
228 content was normalized to the DNA content (GAG/DNA). Each experiment was  
229 performed in duplicate.

230

231     **Immunohistochemistry**

232           Paraffin-embedded sections from cartilage pellets were immersed in 10  
233           mM Tris containing 1 mM EDTA (pH 9.0) and heated at 95 °C for 1 h to retrieve  
234           antigens. The slides were immersed in methanol containing 0.3% H<sub>2</sub>O<sub>2</sub> for 30 min  
235           and then washed with Tris-buffered saline containing 0.1% Tween-20 (TBS-T  
236           buffer). After blocking with 5% normal goat serum, the sections were incubated  
237           overnight at 4 °C with antibody against p16, p21, MMP-13, and IL-6 (1:200; all  
238           from Abcam). After three washes with TBS-T, the sections were incubated with  
239           secondary antibodies conjugated with horseradish peroxidase (Abcam) for 1 h at  
240           room temperature. DAB solution (Dako North America) was then applied for 5  
241           min, and the cells were counterstained with hematoxylin. DAB positive areas in  
242           pellets were quantified using Image J.

243

244     **Statistical analysis**

245           Statistical analysis was performed using SPSS (IBM Corp., Chicago, IL, USA).  
246           Paired-t tests were used for comparison between two groups. One-way analysis  
247           of variance, followed by Tukey's multiple-comparisons test, was used for  
248           comparison between multiple groups. All p values were one-sided, and a p-value

249 < 0.05 was considered statistically significant.

250

251 **Results**

252 **SA- $\beta$ -gal staining**

253 An overview of our experimental design is shown in Fig. 1. We pretreated  
254 OA synovial MSCs with 0.1% DMSO or 20  $\mu$ M ABT-263 for 1 day and then  
255 performed SA- $\beta$ -gal staining to evaluate the proportions of senescent cells. The  
256 optimal concentration of ABT-263 had been determined in a preliminary study  
257 using cells from one donor (Supplementary Fig. 1). Phase contrast and brightfield  
258 images showed the presence of flattened and enlarged cells in the untreated  
259 control group, and those cells showed positive staining for SA- $\beta$ -gal staining (Fig.  
260 2a). By contrast, the culture treated with ABT-263 showed few flattened and  
261 enlarged cells, and the percentage of SA- $\beta$ -gal-positive cells was significantly  
262 lower than in the control group (Fig. 2b,  $p = 3.8 \times 10^{-5}$ ).

263

264 **Apoptosis assay**

265 Early- and late-stage apoptosis was assessed by annexin V/propidium  
266 iodide (PI) staining in control OA synovial MSCs and in OA synovial MSCs treated

267 with ABT-263 (Fig. 3a). The MSCs treated with ABT-263 underwent significantly  
268 greater levels of early-stage apoptosis ( $p = 8.0 \times 10^{-4}$ ), late-stage apoptosis ( $p =$   
269  $3.2 \times 10^{-5}$ ), and total apoptosis ( $p = 2.5 \times 10^{-4}$ ) (Fig. 3b). Co-staining for SA- $\beta$ -gal  
270 and cleaved caspase-3, a molecule with a known pivotal role in the apoptotic  
271 cascade [19], revealed no staining for caspase-3 in the SA- $\beta$ -gal-positive cells of  
272 the control group, whereas the cells in the ABT-263 group were positive for  
273 cleaved caspase-3 (Fig. 3c).

274

## 275 **Colony-forming ability**

276 Colony-forming ability was assessed by culturing 100 pretreated cells for  
277 14 days. Representative images of the colonies stained with crystal violet are  
278 shown in Fig. 4a. The colony numbers were significantly greater in the ABT-263  
279 group than in the control group (Fig. 4b,  $p = 1.5 \times 10^{-3}$ ). The colony diameters  
280 were also significantly larger in the ABT-263 group than in the control group (Fig.  
281 4c,  $p = 9.7 \times 10^{-4}$ ). Histogram distributions of the colony diameters showed a shift  
282 toward larger colonies in response to ABT-263 pretreatment (Supplementary Fig.  
283 2). Most colony-forming cells were small and spindle-shaped, both in the control  
284 and the ABT-263 groups (Fig. 4d). However, the few flattened and enlarged cells

285 that did not form colonies were observed predominantly in the control group (Fig.  
286 4e).

287

288 **Cell surface antigen phenotype**

289 Flow cytometry analyses demonstrated an almost 100% mean rate of  
290 positivity for MSC markers such as CD44, CD73, CD90, and CD105 in both the  
291 control and ABT-263 groups (Fig. 5a), but the difference in the CD90 positive rate  
292 between the control and ABT-263 groups was statistically significant ( $p = 9.0 \times$   
293  $10^{-3}$ ) (Fig. 5b). The mean rates of positivity for the hematopoietic markers CD34  
294 and CD45 were 11.9% in the control group and 3.3% in the ABT-263 group for  
295 CD34 and 0.2% in the control group and 0.1% in the ABT-263 group for CD45.  
296 The positive rate for CD34 was significantly lower in the ABT-263 group than in  
297 the control group ( $p = 0.016$ ).

298

299 **Adipogenic and osteogenic potential**

300 The adipogenic and osteogenic potential of single-cell derived colonies  
301 was investigated by culturing 100 pretreated cells in growth medium for 14 days  
302 to allow colony formation, followed by culture in induction medium for 21 days.

303 Macroscopic images of oil red O and subsequent crystal violet staining are shown  
304 in Fig. 6a. Observation by light microscopy confirmed that pretreatment with ABT-  
305 263 enhanced oil red O staining, indicating increased lipid production by the cells  
306 (Fig. 6b). Quantitative analysis showed that the percentage of oil red O-stained  
307 colonies was significantly higher in the ABT-263 group than in the control group  
308 (Fig. 6c,  $p = 6.4 \times 10^{-4}$ ).

309 Macroscopic images of the cells stained with alizarin red and subsequent  
310 crystal violet staining are shown in Fig. 6d. The cells in both the control and the  
311 ABT-63 groups underwent calcification (Fig. 6e). No significant difference was  
312 detected in the proportion of alizarin red-stained colonies between the control and  
313 ABT-263 groups (Fig. 6f,  $p = 0.070$ ).

314

315 **Chondrogenic potential**

316 Pellets of pretreated cells were cultured for 21 days in chondrogenic  
317 induction medium. The cells formed larger pellets after chondrogenic induction  
318 when pretreated with ABT-263 compared to the control cells (Fig. 7a). The mean  
319 pellet wet weight from the control and ABT-263 groups were 1.9 mg and 4.8 mg,  
320 respectively, confirming a greater pellet mass in the ABT-263 group than in the

321 control group ( $p = 0.052$ ) (Fig. 7b).

322 Biochemical analyses revealed significantly increased GAG amounts ( $p$   
323  $= 9.4 \times 10^{-3}$ ) and a higher GAG/DNA ratio ( $p = 0.013$ ) in the ABT-263 group than  
324 in the control group; however, no significant difference was found in the DNA  
325 amounts between the two groups (Fig. 7b). Safranin o staining was more intense  
326 in the pellets from the ABT-263 group than from the control group (Fig. 7c).

327

### 328 **Immunohistochemistry of chondrogenic pellets**

329 The chondrogenic pellets were immunostained with senescence markers  
330 (p16 and p21) and SASP markers (MMP-13 and IL-6). Representative images  
331 and the ratios of the stained areas are shown in Fig. 8. The percentages of p16,  
332 p21, MMP-13, and IL-6 positive areas group were significantly lower in the ABT-  
333 263 group than in the control group ( $p = 2.1 \times 10^{-3}$ ,  $9.8 \times 10^{-3}$ ,  $5.0 \times 10^{-4}$ , and  $2.5$   
334  $\times 10^{-3}$ , respectively).

335

### 336 **Discussion**

337 In the present study, we demonstrated that senescent cells showing  
338 positive staining for SA- $\beta$ -gal in human synovial MSC samples obtained from OA

339 patients were effectively removed by pretreatment with 20 $\mu$ M ABT-263. Our  
340 apoptosis assay revealed that ABT-263 treatment induced both early- and late-  
341 stage apoptosis in the senescent OA synovial MSCs. In addition, the SA- $\beta$  gal-  
342 positive cells expressed cleaved caspase-3 after the treatment. These results  
343 indicate that ABT-263 could selectively kill senescent cells present in OA synovial  
344 MSC samples by inducing apoptosis. Previous studies have shown that  
345 senescent cells in human chondrocyte and bone marrow derived MSC samples  
346 showed dose-dependent and statistically significantly decreases in the numbers  
347 of SA- $\beta$ -gal-positive cells when treated with ABT-263 [18, 20]. Similar effects of  
348 ABT-263 were also observed in our study. ABT-263 had no adverse effects on  
349 the function of non-senescent MSCs in the present study, but a previous report  
350 indicated that ABT-263 had a cytotoxic effect on bone marrow MSC-derived  
351 osteoblasts both in vitro and in vivo [21].

352 Our colony formation assays indicated that the number and diameter of  
353 colonies were significantly greater in the ABT-263 group than in the untreated  
354 control group. The control group also contained a few colonies with flattened and  
355 enlarged cells, indicative of senescent cells, which are generally growth-arrested  
356 and have enlarged and flattened morphologies [22, 23]. Therefore, our results

357 suggested that senescent cells that have poor colony-forming abilities were  
358 eliminated by the ABT-263 treatment, leaving MSCs with high colony formation  
359 potential in the final culture.

360 Most cells in both groups showed positive immunostaining for CD44,  
361 CD90, and CD105, despite the successful clearing of senescent cells by the ABT-  
362 263 treatment. Consequently, none of these can be considered a candidate for  
363 use as a specific marker for senescent cells. On the contrary, the mean positivity  
364 for CD34 (MSC negative marker) was significantly decreased by ABT-263  
365 treatment, from 11.9% in the control group to 3.3% in the ABT-263 group. A  
366 previous report showed that CD34-positive synovial fibroblasts from OA and  
367 rheumatoid arthritis tissues release high levels of inflammatory cytokines [24].  
368 Similar characteristics are also observed in senescent cells; therefore,  
369 investigating the relationship between CD34 expression and cellular senescence  
370 in the synovium would be an interesting future study.

371 In terms of multipotency, we noted a significant improvement in  
372 adipogenic potential in cells treated with ABT-263, but the osteogenic potential  
373 did not improve. Wagner et al. demonstrated a deterioration in adipogenic  
374 potential in human MSCs with increasing passage number, but did not see an

375 equivalent decline in osteogenesis [25]. However, Bertolo et al. reported opposite  
376 findings [26]. Therefore, no consensus exists regarding the adipogenic and  
377 osteogenic capacities of senescent MSCs. Regarding chondrogenesis, we  
378 observed that the synovial MSCs pretreated with ABT-263 formed cartilaginous  
379 pellets rich in GAGs and showed decreased expression of senescence markers  
380 and SASP factors. Therefore, these cells are expected to induce better cartilage  
381 regeneration than untreated cells by producing more cartilage matrix and  
382 releasing fewer of the catabolic factors that deteriorate the functions of the  
383 surrounding cells. Our study had one significant limitation, as we did not  
384 investigate the *in vivo* therapeutic effect of ABT-263–treated MSCs. Further  
385 research using animal models of cartilage/meniscus injury or OA is needed to  
386 verify our results.

387           MSCs are a heterogeneous population, so purification is sometimes  
388 carried out to isolate true stem cells [27]. MSCs are typically purified by  
389 fluorescence-activated cell sorting (FACS) [28], but the lack of specific surface  
390 markers for senescent cells limits this approach [29]. We propose that the  
391 purification of MSCs could be improved by administration of a senolytic agent,  
392 such as ABT-263. Care would be needed when using ABT-263 in terms of

393 cytotoxic effects; however, when compared with FACS, ABT-263 pretreatment is  
394 easy, inexpensive, and requires no special equipment. Senescence of various  
395 MSC types is also known to be accelerated during aging of individuals and during  
396 in vitro serial passaging of MSCs in culture [25, 30]. ABT-263 pretreatment could  
397 also be beneficial in these cases.

398

### 399 **Conclusions**

400 Pretreatment with ABT-263 selectively eliminated senescent cells in  
401 synovial MSCs derived from OA patients. The pretreated MSCs consistently  
402 showed higher colony formation, adipogenic, and chondrogenic abilities, and  
403 decreased SASP expression. These results indicate that ABT-263 could be a  
404 useful senolytic drug to improve the function of synovial MSCs obtained from OA  
405 patients and could hold promise for the development of effective cell-based OA  
406 therapy.

407

### 408 **Abbreviations**

409 α-MEM: α-modified essential medium; DAB: Diaminobenzidine; DMSO: Dimethyl  
410 sulfoxide; FACS: Fluorescence-activated cell sorting; GAG: Glycosaminoglycan;

411 ITS: Insulin-transferrin-selenium; IL-6: Interleukin-6; MRI: Magnetic resonance  
412 imaging; MMP-13: Matrix metalloprotease-13; MSCs: Mesenchymal stem cells;  
413 OA: Osteoarthritis; PBS: Phosphate buffered saline; PI: Propidium iodide; SASP:  
414 Senescence-associated secretory phenotype; SA- $\beta$ -gal: Senescence associated  
415  $\beta$ -galactosidase

416

417 **Declarations**

418 **Ethics approval and consent to participate**

419 This study was approved by the Medical Research Ethics Committee of  
420 Tokyo Medical and Dental University, and written informed consent was obtained  
421 from all donors.

422

423 **Consent for publication**

424 Not applicable.

425

426 **Availability of data and materials**

427 The datasets generated and analyzed during the current study are  
428 available from the corresponding author on reasonable request.

429

430 **Competing interests**

431 The authors declare that they have no competing interests.

432

433 **Fundings**

434 This study was supported by the Japan Society for the Promotion of

435 Science (JSPS) KAKENHI (20K17990).

436

437 **Authors' contributions**

438 YM provided ideas, performed all experiments, and wrote the manuscript.

439 KE designed the study, provided ideas, organized the data, and completed the

440 manuscript. KK provided ideas, contributed to acquisition of data, and revised the

441 manuscript. IS provided ideas and revised the manuscript. All authors read and

442 approved the submitted draft of the paper.

443

444 **Acknowledgements**

445 The authors thank Nobutake Ozeki, Mitsuru Mizuno, and Hisako Katano

446 for their advice and support. The authors also thank Hideyuki Koga for the

447 provision of human tissues, Kimiko Takanashi for managing our laboratory, and  
448 Ellen Roider for English editing.

449

450 **References**

- 451 1 Jeon OH, David N, Campisi J, Elisseeff JH. Senescent cells and  
452 osteoarthritis: a painful connection. *J Clin Invest.* 2018;128(4):1229-37.
- 453 2 Sellam J, Berenbaum F. The role of synovitis in pathophysiology and  
454 clinical symptoms of osteoarthritis. *Nat Rev Rheumatol.* 2010;6(11):625-  
455 35.
- 456 3 Taruc-Uy RL, Lynch SA. Diagnosis and treatment of osteoarthritis. *Prim  
457 Care.* 2013;40(4):821-36, vii.
- 458 4 Bianco P, Robey PG, Simmons PJ. Mesenchymal stem cells: revisiting  
459 history, concepts, and assays. *Cell Stem Cell.* 2008;2(4):313-9.
- 460 5 Barry F. MSC Therapy for Osteoarthritis: An Unfinished Story. *J Orthop  
461 Res.* 2019;37(6):1229-35.
- 462 6 Sakaguchi Y, Sekiya I, Yagishita K, Muneta T. Comparison of human stem  
463 cells derived from various mesenchymal tissues: superiority of synovium  
464 as a cell source. *Arthritis Rheum.* 2005;52(8):2521-9.

- 465 7 Yoshimura H, Muneta T, Nimura A, Yokoyama A, Koga H, Sekiya I.
- 466 Comparison of rat mesenchymal stem cells derived from bone marrow,
- 467 synovium, periosteum, adipose tissue, and muscle. *Cell Tissue Res.*
- 468 2007;327(3):449-62.
- 469 8 Mochizuki T, Muneta T, Sakaguchi Y, Nimura A, Yokoyama A, Koga H, et
- 470 al. Higher chondrogenic potential of fibrous synovium- and adipose
- 471 synovium-derived cells compared with subcutaneous fat-derived cells:
- 472 distinguishing properties of mesenchymal stem cells in humans. *Arthritis*
- 473 *Rheum.* 2006;54(3):843-53.
- 474 9 De Bari C, Dell'Accio F, Tylzanowski P, Luyten FP. Multipotent
- 475 mesenchymal stem cells from adult human synovial membrane. *Arthritis*
- 476 *Rheum.* 2001;44(8):1928-42.
- 477 10 Koga H, Muneta T, Nagase T, Nimura A, Ju YJ, Mochizuki T, et al.
- 478 Comparison of mesenchymal tissues-derived stem cells for in vivo
- 479 chondrogenesis: suitable conditions for cell therapy of cartilage defects
- 480 in rabbit. *Cell Tissue Res.* 2008;333(2):207-15.
- 481 11 Horie M, Driscoll MD, Sampson HW, Sekiya I, Caroom CT, Prockop DJ,
- 482 et al. Implantation of allogenic synovial stem cells promotes meniscal

- 483 regeneration in a rabbit meniscal defect model. *J Bone Joint Surg Am.*  
484 2012;94(8):701-12.
- 485 12 Ozeki N, Muneta T, Koga H, Nakagawa Y, Mizuno M, Tsuji K, et al. Not  
486 single but periodic injections of synovial mesenchymal stem cells  
487 maintain viable cells in knees and inhibit osteoarthritis progression in rats.  
488 *Osteoarthritis Cartilage.* 2016;24(6):1061-70.
- 489 13 Sekiya I, Katano H, Mizuno M, Koga H, Masumoto J, Tomita M, et al.  
490 Alterations in cartilage quantification before and after injections of  
491 mesenchymal stem cells into osteoarthritic knees. *Sci Rep.*  
492 2021;11(1):13832.
- 493 14 van Deursen JM. The role of senescent cells in ageing. *Nature.*  
494 2014;509(7501):439-46.
- 495 15 Del Rey MJ, Valín Á, Usategui A, Ergueta S, Martín E, Municio C, et al.  
496 Senescent synovial fibroblasts accumulate prematurely in rheumatoid  
497 arthritis tissues and display an enhanced inflammatory phenotype.  
498 *Immun Ageing.* 2019;16:29.
- 499 16 Huang J, Chen C, Liang C, Luo P, Xia G, Zhang L, et al. Dysregulation of  
500 the Wnt Signaling Pathway and Synovial Stem Cell Dysfunction in

- 501 Osteoarthritis Development. Stem Cells Dev. 2020;29(7):401-13.
- 502 17 Zhang L, Pitcher LE, Prahalad V, Niedernhofer LJ, Robbins PD. Targeting
- 503 Cellular Senescence with Senotherapeutics: Senolytics and
- 504 Senomorphics. Febs j. 2022.
- 505 18 Grezella C, Fernandez-Rebollo E, Franzen J, Ventura Ferreira MS, Beier
- 506 F, Wagner W. Effects of senolytic drugs on human mesenchymal stromal
- 507 cells. Stem Cell Res Ther. 2018;9(1):108.
- 508 19 Gown AM, Willingham MC. Improved detection of apoptotic cells in
- 509 archival paraffin sections: immunohistochemistry using antibodies to
- 510 cleaved caspase 3. J Histochem Cytochem. 2002;50(4):449-54.
- 511 20 Yang H, Chen C, Chen H, Duan X, Li J, Zhou Y, et al. Navitoclax (ABT263)
- 512 reduces inflammation and promotes chondrogenic phenotype by clearing
- 513 senescent osteoarthritic chondrocytes in osteoarthritis. Aging (Albany
- 514 NY). 2020;12(13):12750-70.
- 515 21 Sharma AK, Roberts RL, Benson RD, Jr., Pierce JL, Yu K, Hamrick MW,
- 516 et al. The Senolytic Drug Navitoclax (ABT-263) Causes Trabecular Bone
- 517 Loss and Impaired Osteoprogenitor Function in Aged Mice. Front Cell
- 518 Dev Biol. 2020;8:354.

- 519 22 Hayflick L, Moorhead PS. The serial cultivation of human diploid cell  
520 strains. *Exp Cell Res.* 1961;25:585-621.
- 521 23 Shirasawa S, Sekiya I, Sakaguchi Y, Yagishita K, Ichinose S, Muneta T.  
522 In vitro chondrogenesis of human synovium-derived mesenchymal stem  
523 cells: optimal condition and comparison with bone marrow-derived cells.  
524 *J Cell Biochem.* 2006;97(1):84-97.
- 525 24 Mizoguchi F, Slowikowski K, Wei K, Marshall JL, Rao DA, Chang SK, et  
526 al. Functionally distinct disease-associated fibroblast subsets in  
527 rheumatoid arthritis. *Nat Commun.* 2018;9(1):789.
- 528 25 Wagner W, Horn P, Castoldi M, Diehlmann A, Bork S, Saffrich R, et al.  
529 Replicative senescence of mesenchymal stem cells: a continuous and  
530 organized process. *PLoS One.* 2008;3(5):e2213.
- 531 26 Bertolo A, Baur M, Guerrero J, Pötzl T, Stoyanov J. Autofluorescence is  
532 a Reliable in vitro Marker of Cellular Senescence in Human Mesenchymal  
533 Stromal Cells. *Sci Rep.* 2019;9(1):2074.
- 534 27 Zha K, Li X, Yang Z, Tian G, Sun Z, Sui X, et al. Heterogeneity of  
535 mesenchymal stem cells in cartilage regeneration: from characterization  
536 to application. *NPJ Regen Med.* 2021;6(1):14.

537 28 Gullo F, De Bari C. Prospective purification of a subpopulation of human  
538 synovial mesenchymal stem cells with enhanced chondro-osteogenic  
539 potency. *Rheumatology (Oxford)*. 2013;52(10):1758-68.

540 29 Scudellari M. To stay young, kill zombie cells. *Nature*.  
541 2017;550(7677):448-50.

542 30 Kapetanos K, Asimakopoulos D, Christodoulou N, Vogt A, Khan W.  
543 Chronological Age Affects MSC Senescence In Vitro-A Systematic  
544 Review. *Int J Mol Sci*. 2021;22(15).

545

546 **Figure legends**

547 **Fig. 1. Scheme of the experiments.** Synovial mesenchymal stem cells (MSCs)  
548 from osteoarthritis (OA) patients were treated with 0.1% dimethyl sulfoxide  
549 (DMSO) or 20  $\mu$ M ABT-263 in DMSO for 24 h. After the treatment, the cells were  
550 expanded for another 6 days and used for the experiments. Apoptosis assays  
551 were performed immediately after the treatment.

552

553 **Fig. 2 Senescence-associated beta galactosidase (SA- $\beta$  gal) staining.** (a)  
554 Phase contrast and brightfield images. (b) The ratio of SA- $\beta$  gal-positive cells in

555 control and ABT-263 group.

556

557 **Fig. 3. Apoptosis assay.** (a) Flow cytometry analysis of Annexin V/propidium

558 iodide (PI). Dot plots show the percentages of viable (Q4), early apoptotic (Q3),

559 and late apoptotic (Q2) cells. (b) The ratio of early, late, and total apoptotic cells

560 in the control and ABT-263 groups. (c) Co-staining of senescence-associated

561 beta galactosidase (blue) and cleaved caspase-3 (brown) after the treatment with

562 ABT-263.

563

564 **Fig. 4. Colony-forming ability.** (a) Representative images of colonies stained

565 with crystal violet (4 replicate dishes per donor). (b) Colony numbers per dish in

566 the control and ABT-263 groups. (c) Diameter of colonies in the control and ABT-

567 263 groups. (d) Representative image of colony-forming cells. (e) Representative

568 image of flattened and enlarged cells that did not form colonies.

569

570 **Fig. 5. Surface antigen expression.** (a) Representative flow cytometry

571 histograms. Red solid lines indicate the control group and green solid lines

572 indicate the ABT-263 group. Dotted lines show the isotype control. (b) The

573 expression rate of each surface antigen. Values are shown as mean  $\pm$  SD from 5  
574 donors.

575

576 **Fig. 6. Adipogenic and osteogenic differentiation.** (a) Representative images  
577 of oil red O and crystal violet (CV) staining (3 replicate dishes per donor). (b) The  
578 percentage of oil red O-stained colonies in the control and ABT-263 groups. (c)  
579 Representative images of alizarin red and CV staining (3 replicate dishes per  
580 donor). (d) The percentage of alizarin red-stained colonies in the control and ABT-  
581 263 groups.

582

583 **Fig. 7. Chondrogenic differentiation.** (a) Gross appearance of chondrogenic  
584 pellets (5 or 6 replicate pellets per donor). (b) Pellet wet weight, DNA  
585 quantification, glycosaminoglycan (GAG) quantification, and GAG/DNA ratio (3 or  
586 4 replicate pellets per donor). (c) Representative images of safranin O staining of  
587 chondrogenic pellets.

588

589 **Fig. 8. Immunohistochemistry of senescence markers in chondrogenic  
590 pellets.** Representative images and positive ratios of (a) p16, (b) p21, (c) MMP-

591 13, and (d) IL-6 immunostaining in the control and ABT-263 groups.

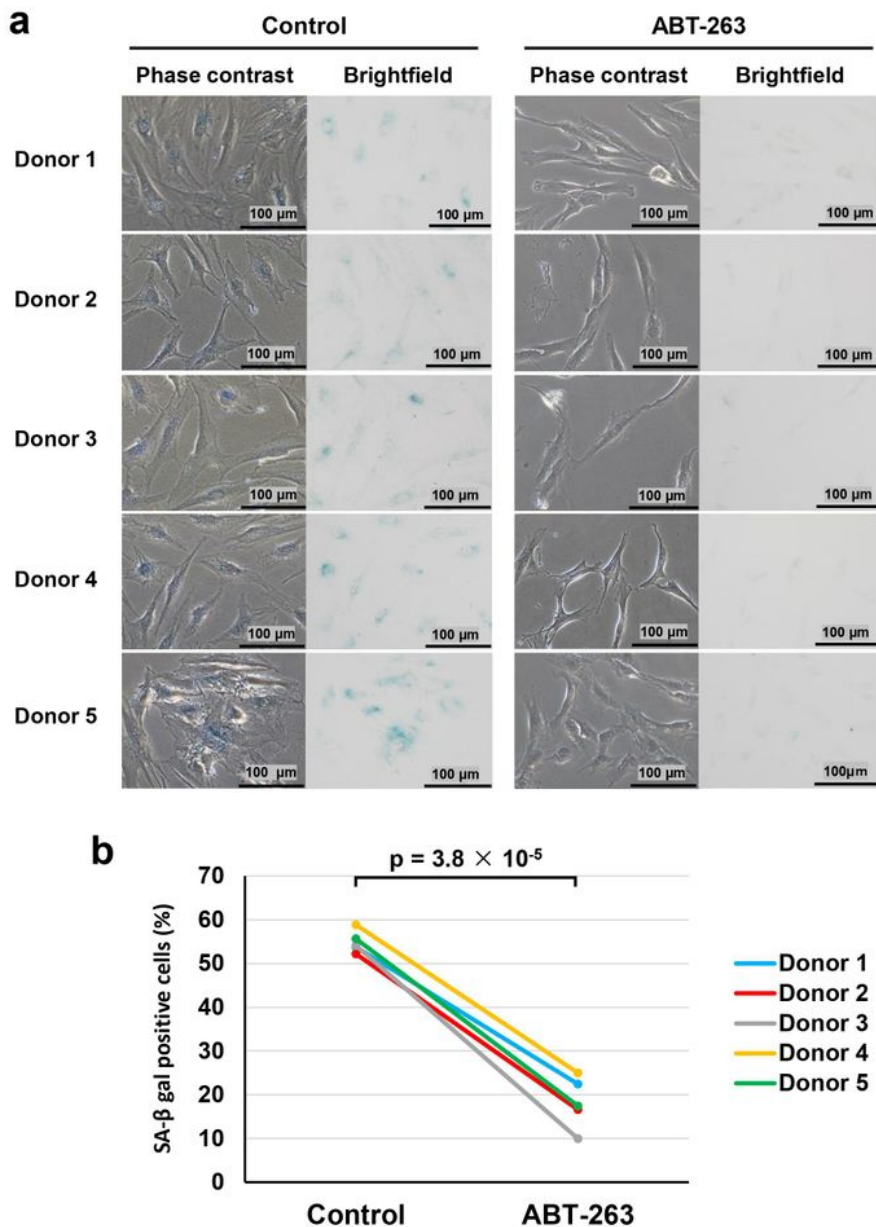
# Figures



## Figure 1

Scheme of the experiments. Synovial mesenchymal stem cells (MSCs) from osteoarthritis (OA) patients were treated with 0.1% dimethyl sulfoxide (DMSO) or 20  $\mu$ M ABT-263 in DMSO for 24 h. After the treatment, the cells were expanded for another 6 days and used for the experiments. Apoptosis assays were performed immediately after the treatment.

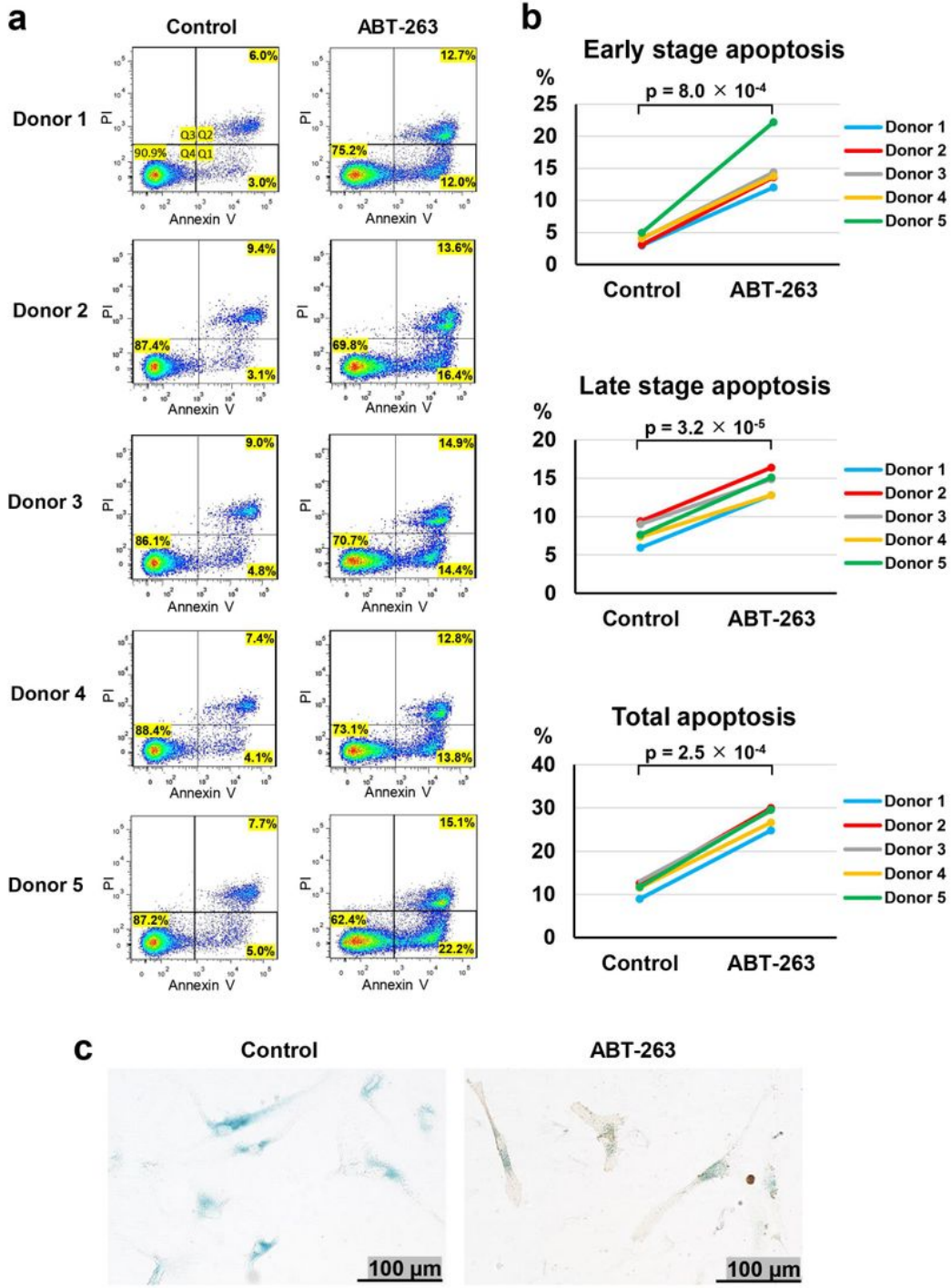
**Fig. 2**



**Figure 2**

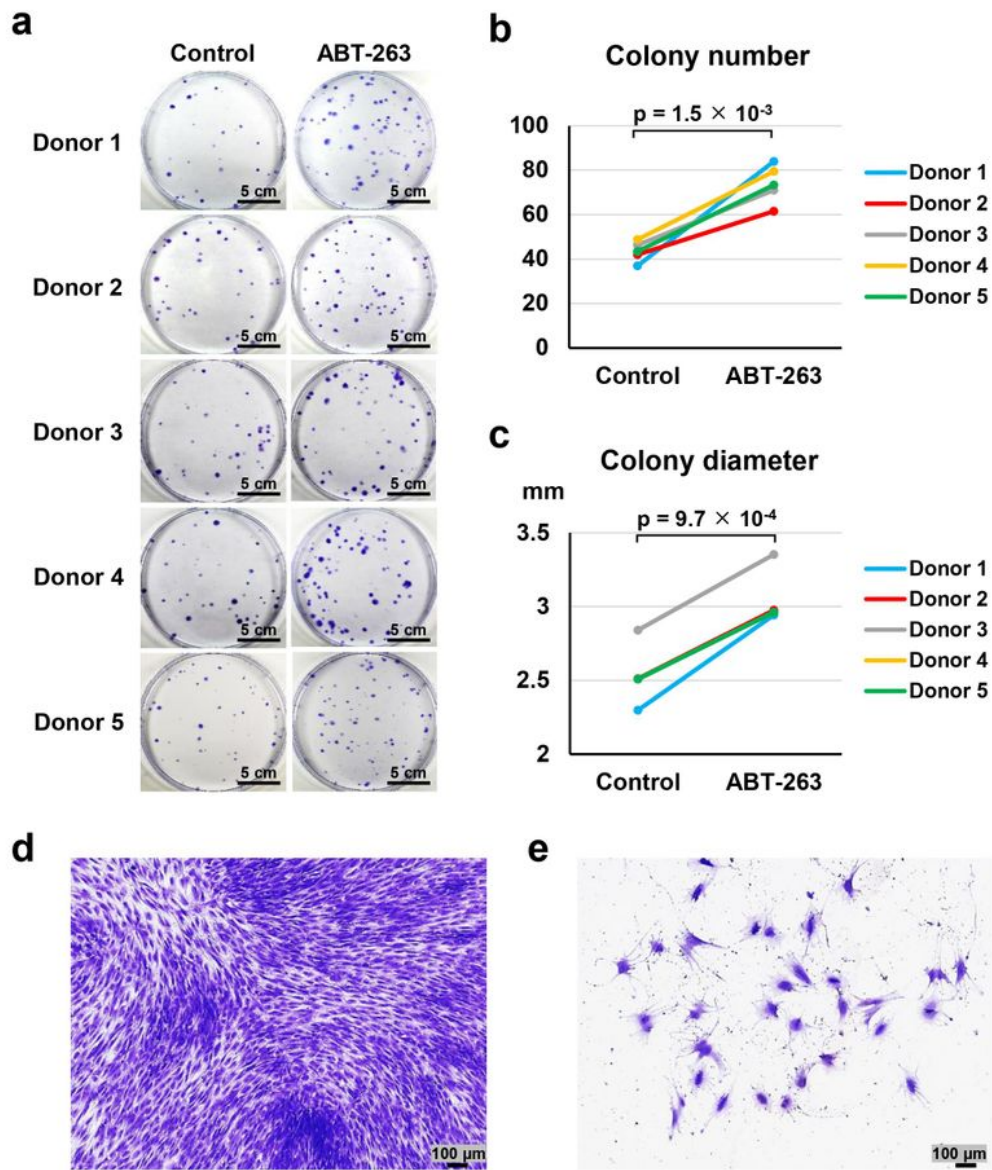
Senescence-associated beta galactosidase (SA- $\beta$  gal) staining. (a) Phase contrast and brightfield images. (b) The ratio of SA- $\beta$  gal-positive cells in control and ABT-263 group.

# Fig. 3

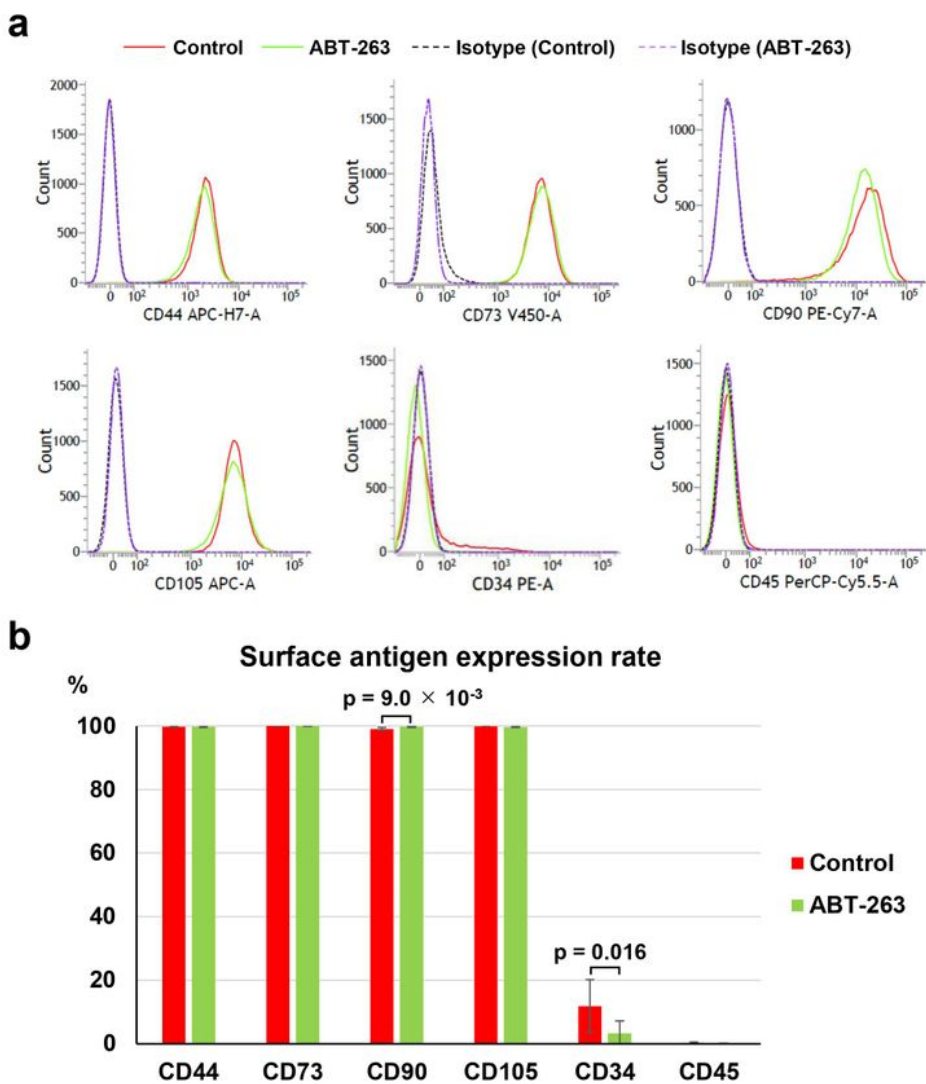


## Figure 3

Apoptosis assay. (a) Flow cytometry analysis of Annexin V/propidium iodide (PI). Dot plots show the percentages of viable (Q4), early apoptotic (Q3), and late apoptotic (Q2) cells. (b) The ratio of early, late, and total apoptotic cells in the control and ABT-263 groups. (c) Co-staining of senescence-associated beta galactosidase (blue) and cleaved caspase-3 (brown) after the treatment with ABT-263.

**Fig. 4****Figure 4**

Colony-forming ability. (a) Representative images of colonies stained with crystal violet (4 replicate dishes per donor). (b) Colony numbers per dish in the control and ABT-263 groups. (c) Diameter of colonies in the control and ABT-263 groups. (d) Representative image of colony-forming cells. (e) Representative image of flattened and enlarged cells that did not form colonies.

**Fig. 5****Figure 5**

Surface antigen expression. (a) Representative flow cytometry histograms. Red solid lines indicate the control group and green solid lines indicate the ABT-263 group. Dotted lines show the isotype control. (b) The expression rate of each surface antigen. Values are shown as mean  $\pm$  SD from 5 donors.

**Fig. 6**

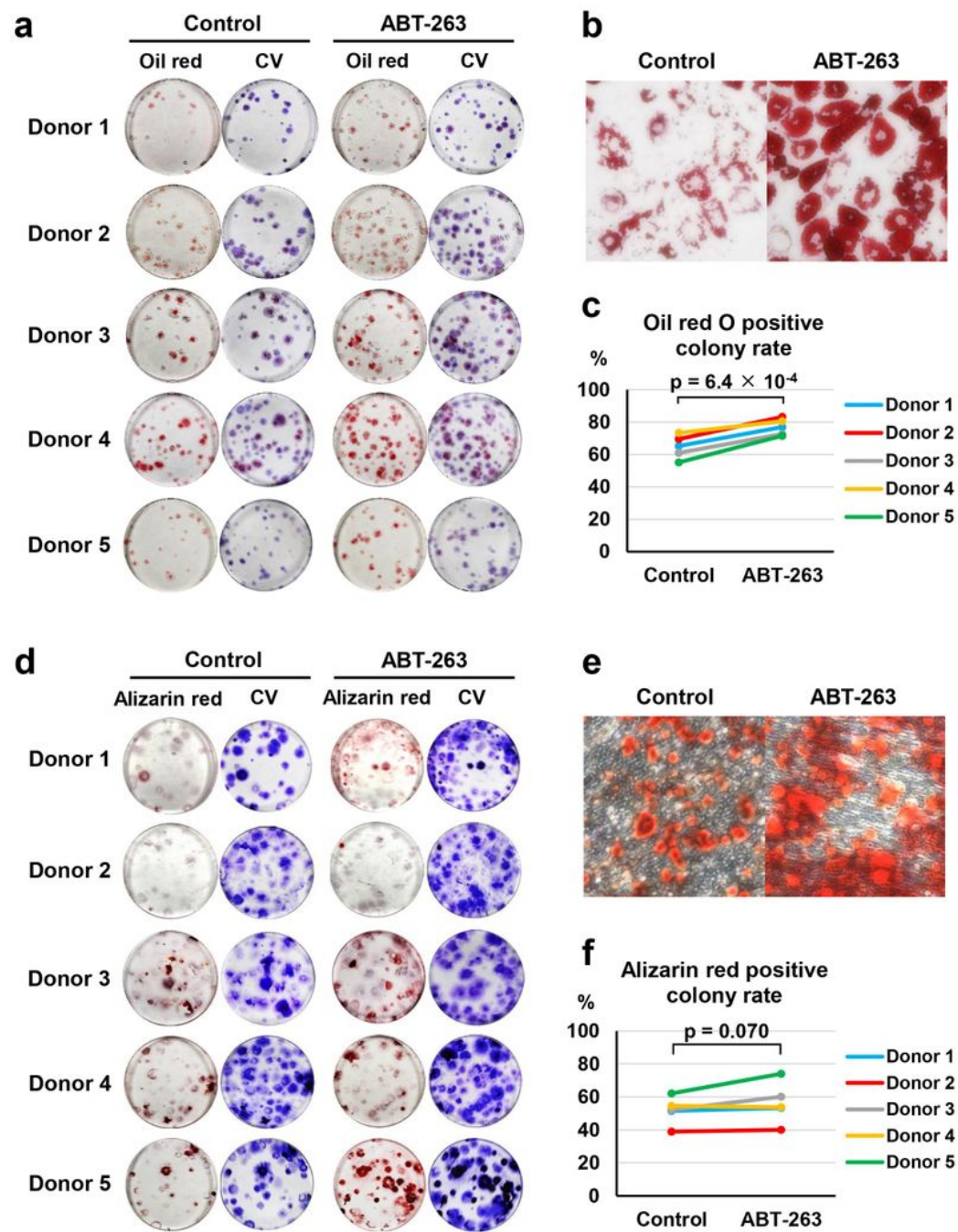


**Figure 6**

Adipogenic and osteogenic differentiation. (a) Representative images of oil red O and crystal violet (CV) staining (3 replicate dishes per donor). (b) The percentage of oil red O-stained colonies in the control and ABT-263 groups. (c) Representative images of alizarin red and CV staining (3 replicate dishes per donor). (d) The percentage of alizarin red-stained colonies in the control and ABT-263 groups.

**Fig. 7**

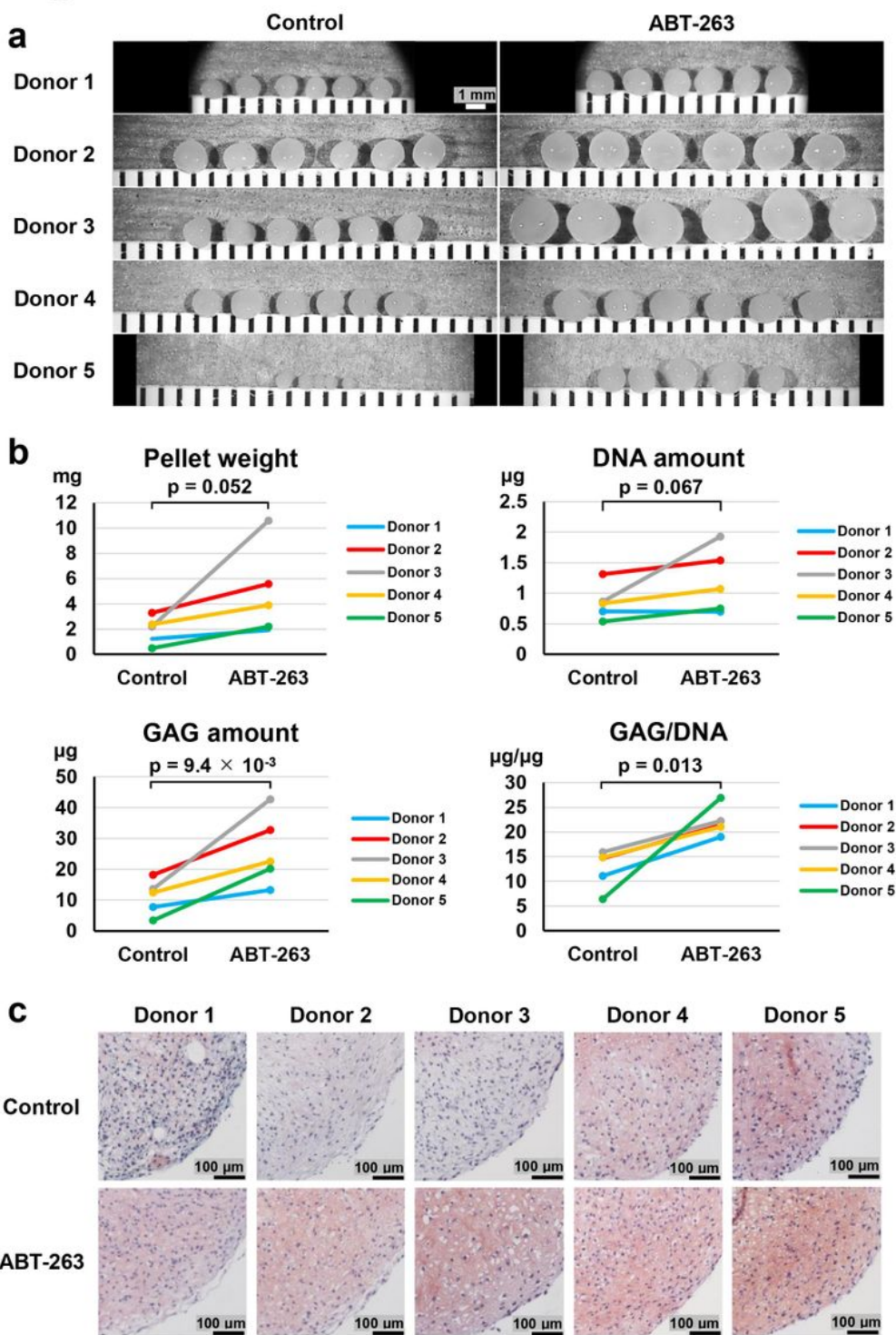


**Figure 7**

Chondrogenic differentiation. (a) Gross appearance of chondrogenic pellets (5 or 6 replicate pellets per donor). (b) Pellet wet weight, DNA quantification, glycosaminoglycan (GAG) quantification, and GAG/DNA ratio (3 or 4 replicate pellets per donor). (c) Representative images of safranin O staining of chondrogenic pellets.

# Fig. 8

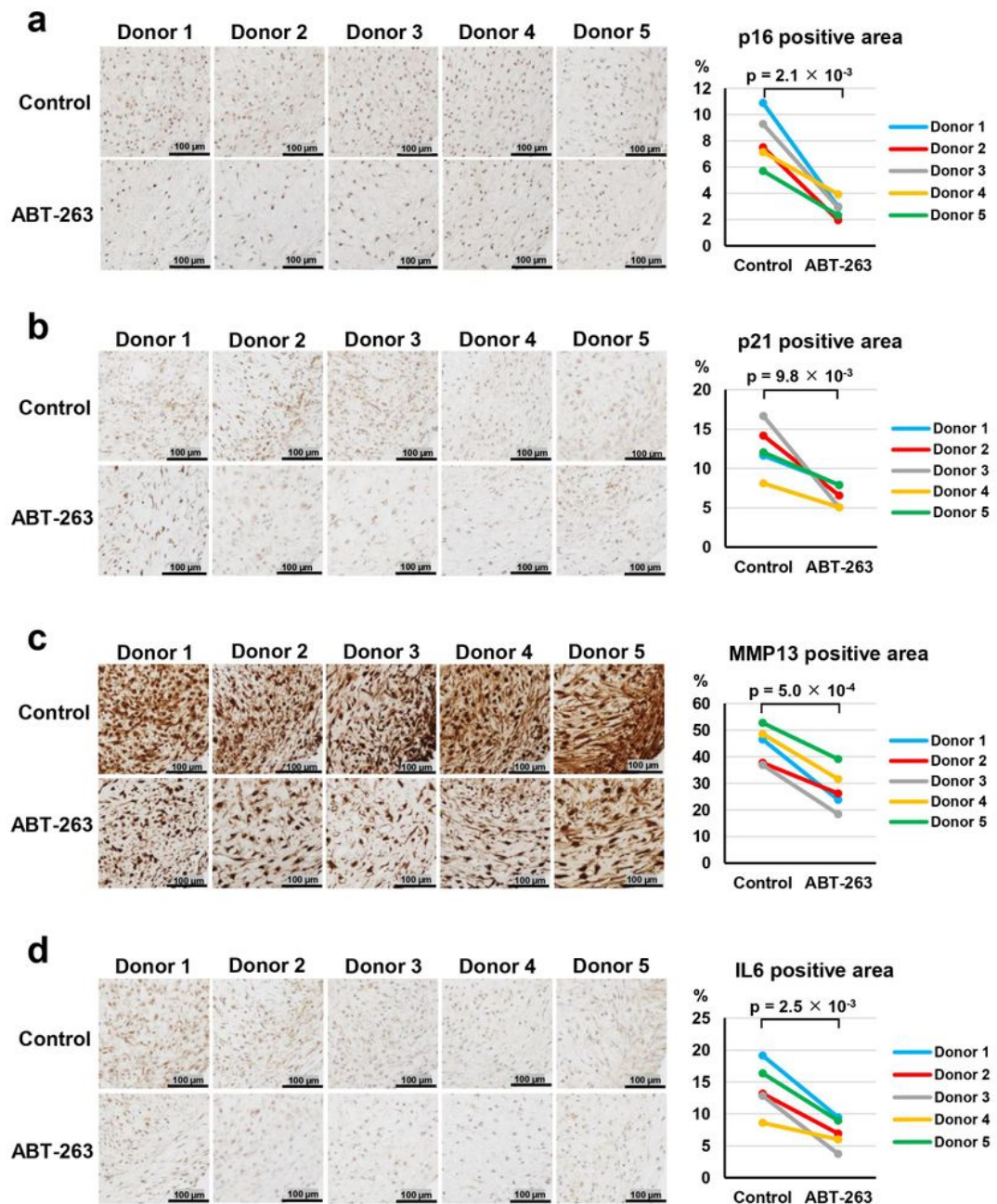


## Figure 8

Immunohistochemistry of senescence markers in chondrogenic pellets. Representative images and positive ratios of (a) p16, (b) p21, (c) MMP- 13, and (d) IL-6 immunostaining in the control and ABT-263 groups

## Supplementary Files

This is a list of supplementary files associated with this preprint. Click to download.

- [SCRTABT263SupplementalFigures220228.pdf](#)